Taylor & Francis
Taylor & Francis Group

Check for updates

Searching for potential drugs against SARS-CoV-2 through virtual screening on several molecular targets

Joyce S. F. D. Almeida[a], Fernanda D. Botelho[a], Felipe R. de Souza[b], Marcelo C. dos Santos[a], Arlan da Silva Goncalves[c,d], Rodrigo L. B. Rodrigues[e], Monique Cardozo[f], Daniel A. S. Kitagawa[a], Leandro A. Vieira[a], Raphael S. F. Silva[a,g], Samir F. A. Cavalcante[f#], Leonardo da C. Bastos[a], Mariana de O. T. Nogueira[a], Priscila I. R. de Santana[a], Juliana de O. C. Brum[a], Eugenie Nepovimova[h], Kamil Kuca[h], Steven R. LaPlante[i], Erick B. F. Galante[e] and Tanos C. C. Franca[a,h,i]

aLaboratory of Molecular Modeling Applied to Chemical and Biological Defense (LMCBD), Military Institute of Engineering, Rio de Janeiro/RJ, Brazil; bDepartment of Chemistry, Pontifical Catholic University of Rio de Janeiro, Rio de Janeiro/RJ, Brazil; cDepartment of Chemistry, Federal Institute of Espírito Santo - Unit Vila Velha, Vila Velha/ES, Brazil; dPPGQUI (Graduate Program in Chemistry), Federal University of Espirito Santo, Vitoria/ES, Brazil; eDepartment of Chemical Engineering, Instituto Militar de Engenharia, Rio de Janeiro/RJ, Brazil; fInstitute of Chemical, Biological, Radiological and Nuclear Defense (IDQBRN), Brazilian Army Technological Center (CTEx), Rio de Janeiro/RJ, Brazil; gCoordination of Chemistry, Federal Institute of Education Science and Technology of Rio de Janeiro, Rio de Janeiro/RJ, Brazil; hFaculty of Science, Department of Chemistry, University of Hradec Kralove, Hradec Kralove, Czech Republic; iINRS, Centre Armand-Frappier Santé Biotechnologie 531, Boulevard des Prairies, Laval, QC, Canada

Communicated by Ramaswamy H. Sarma

ABSTRACT

The acute respiratory syndrome caused by the SARS-CoV-2, known as COVID-19, has been ruthlessly tormenting the world population for more than six months. However, so far no effective drug or vaccine against this plague have emerged yet, despite the huge effort in course by researchers and pharmaceutical companies worldwide. Willing to contribute with this fight to defeat COVID-19, we performed a virtual screening study on a library containing Food and Drug Administration (FDA) approved drugs, in a search for molecules capable of hitting three main molecular targets of SARS-CoV-2 currently available in the Protein Data Bank (PDB). Our results were refined with further molecular dynamics (MD) simulations and MM-PBSA calculations and pointed to 7 multi-target hits which we propose here for experimental evaluation and repurposing as potential drugs against COVID-19. Additional rounds of docking, MD simulations and MM-PBSA calculations with remdesivir suggested that this compound can also work as a multi-target drug against SARS-CoV-2.

Introduction

According to the literature SARS-CoV-2 belongs to the coronavirus family which has been around and causing pandemics for a while. However, this time the infection caused, called COVID-19, is a bit worse and capable of collapsing the lungs very quickly, killing the patient if no respiratory support is provided, being declared a worldwide pandemic in 11 March 2020 by the World Health Organization (WHO). In most countries the shortage of enough respirators, as well as, specialized personal to operate them, aroused a big fear of collapsing in the health systems. Therefore, social distancing and/or lockdown of the entire population was the most immediate response to this situation in order of smoothing the progress curve of the disease, and saving the Governments some time for preparing their health systems for facing properly this pandemic (Bedford et al., 2020; Cucinotta & Vanelli, 2020; Ortiz-Prado et al. 2020; Velavan & Meyer, 2020).

However, improving the health infrastructure is not enough and the situation will be totally under control only after the naturally achieving of herd immunity by the population, the development of a vaccine, or emergence of a drug capable of avoiding the respiratory complications of COVID-19 (Fierabracci et al., 2020; Gates, 2020). As the first two options can take months, maybe more than a year, the most immediate solution to beat COVID-19 is the search for new drugs based on the repurposing approach (Pushpakom et al., 2019). On this sense we performed a comprehensive virtual screening (VS) study on a library comprising FDA approved drugs in a search for molecules capable of hitting the three main molecular targets of SARS-CoV-2 currently available in the protein data bank (PDB) (https://www.rcsb.org/) (Berman et al., 2000a).

In order to select which proteins would be studied in terms of their interactions with small molecules, we analyzed the role that different proteins play in SARS-CoV-2 mechanisms of replication or cell entrance, and the availability and quality of their

Table 1. Protein structures retrieved for the PDB (Berman et al., 2000b) for this study.

PDB Code	Protein	Abbreviation used in this work	Binding pocket	Residues	References
6XMK	SARS-CoV-2 main protease in complex with the inhibitor 7j ($IC_{50} = 0.45\,\mu M$)	$SC2M^{pro}$	Active site	Gly143, Cys145, His163, His164, Glu166, Gln189, Thr190	(Rathnayake et al., 2020)
7CMD	Papain-like protease of SARS CoV-2 in complex with the inhibitor GRL0617 ($IC_{50} = 2.2\,\mu M$)	$SC2PL^{pro}$	Active site	Cys111, Gly163, Asp164, Tyr264, Tyr268, Gly271, His272, Asp286	(Gao et al., 2020)
7JZU	SARS-CoV-2 spike in complex with the peptide LCB1 ($IC_{50} = 23.5\,pM$)	$SC2Spyke$	RBD	Lys417, Gly446, Tyr449, Tyr453, Leu455, Phe456, Ala475, Phe486, Asn487, Tyr489, Gln493, Gly496, Gln498, Thr500, Asn501, Gly502, Tyr505	(Cao et al., 2020)

three-dimensional structures in the PDB (https://www.rcsb.org/) (Berman et al., 2000a). All selected proteins are part of the viral machinery responsible for the replication and transcription of SARS-CoV-2 RNA genome or play important roles in the viral mechanisms of entrance inside human cells. Main protease (M^{pro}) is responsible for proteolysis of polyproteins 1a and 1ab, generating smaller proteins that are necessary for the virus replication (Jin et al., 2020; Rathnayake et al., 2020). Spyke protein is a homotrimer located in the external surface of the virus and contains the receptor-binding domain (RBD), which directly binds to the peptidase domain of the angiotensin-converting enzyme 2 (ACE2), and consequently promotes the entrance of the virus inside the cell (Cao et al., 2020; Yan et al., 2020). Finally, papain-like protease (PL^{pro}) is responsible for processing the viral polyprotein, a process that is required for the release and maturation of several non-structural proteins, and thus is essential for the replication of SARS-CoV-2 and other coronaviruses (Báez-Santos et al., 2015; Gao et al., 2020; Klemm et al., 2020).

Our search screened 1930 compounds contained in the FDA-approved drugs data set available at the Cheminformatic tools and Databases server (ChemoInfo) (https://chemoinfo.ipmc.cnrs.fr/) (Douguet, 2010, 2018) against the targets cited above, and the 50 best molecules were selected for further docking studies using Molegro Virtual Docker (MVD®) 6.0 (Thomsen & Christensen, 2006), in order to confirm their potential for drug repurposing against COVID-19. The 7 drugs that showed potential to bind the three protein targets selected in this study were submitted to molecular dynamics (MD) simulations and MM-PBSA calculations in order to corroborate the docking results. We also performed the same theoretical studies for remdesivir in complex with each target protein, since this drug has been reported in literature as presenting promising *in silico* and experimental results for the treatment of patients with COVID-19 (Grein et al., 2020; Hendaus, 2020; Naik et al., 2020; Wang et al., 2020).

Methodology

Virtual screening studies

Targets and search space
The molecular targets selected from the PDB (Berman et al., 2000b) and their respective binding pockets chosen to run

Table 2. Coordinates and radius of the search spaces of each target.

Protein name	Coordinates			Radius (Å)
	X	Y	Z	
$SC2M^{pro}$	−13.26	12.64	69.06	13.0
$SC2PL^{pro}$	−30.98	21.76	30.14	15.0
$SC2SPyke$	179.46	119.64	251.82	24.0

the VS study, are listed on Table 1. The search space of each molecular target in Table 1 were centered in the respective co-crystalized ligands.

The spherical search spaces for the VS studies on each target were determined with MVD® (Thomsen & Christensen, 2006) as centered in the respective binding pockets defined in Table 1. The coordinates and radius used for each search are listed in Table 2.

Libraries
As mentioned above we used the FDA-approved drugs data set (called here FDA-library) available at ChemoInfo server (https://chemoinfo.ipmc.cnrs.fr/) that provided 1930 FDA-approved drugs ready for docking (Douguet, 2010, 2018). Those molecules were evaluated regarding their interactions with each of the protein targets listed in Table 1.

Receptor-based virtual screening (RBVS)
A Receptor-based Virtual Screening (RBVS) was carried out for each target protein separately using the ChemoInfo VS tool, which employs the docking algorithm Protein-Ligand ANT System (PLANTS) (Korb et al., 2009). For each target protein, the respective .pdb file and coordinates of the center of the binding site, as defined in Table 2, were given as inputs. After evaluation of the FDA-library, the ChemoInfo VS tool returned the results consisting on a list of the molecules ranked by the PLANTS (Korb et al., 2009) scoring function. The top results correspond to molecules that stablished the most favorable interactions with the target.

For each target, the best 50 results returned by the ChemoInfo VS tool were retrieved and these results were filtered in order to remove drugs that mainly act in the central and/or peripheral nervous system, renal system and/or cardiovascular system, because these effects would make it
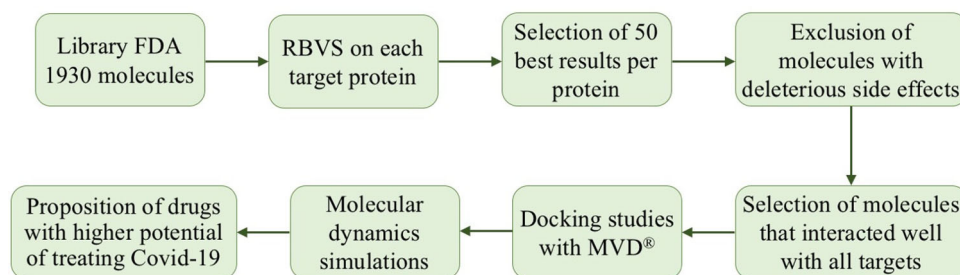
Figure 1. Flowchart of the VS study.

impossible to use those types of drugs in patients infected with COVID-19. After the filtering, we looked for drugs that showed potential to interact with more than one target protein and, therefore, triggering a synergistic effect, enhancing their potential to stop or slow down the SARS-CoV-2 action inside the human body. The drugs were then reranked in decreasing order of the number of protein targets that they interacted favorably with and, the ones showing favorable interactons with the three targets, were submitted to MVD® and rounds of MD simulation and MM-PBSA calculations. A flowchart summarizing the VS procedure used in this study is illustrated in Figure 1.

Docking studies

The drugs that showed favorable interactions with all three targets selected in this work were submitted to MVD®, using the same protocol validated before (Botelho et al., 2020), in order to re-evaluate the protein-ligand interactions using the Moldock Score, a docking algorithm more accurate than PLANTS (Korb et al., 2009). For this task their 3 D structures were constructed in the Spartan 08 software (Hehre et al., 2006), using the semi-empirical method Parametric Method 3 (PM3) (Stewart, 2004) for geometry optimization, and the Natural Population Analysis (NPA) (Reed et al., 1985) method for atomic charges calculations.

For each protein-ligand complex, 10 runs were carried out in the search spaces defined in Table 2, with 30 poses returned for each run. Those poses were analyzed regarding their MolDock Score and the residues they formed hydrogen bonds (H-bonds) with. After, the best pose of each drug in each target was selected to be submitted to MD simulations and MM-PBSA calculations. The complexes remdesivir/targets were also generated with MVD®, following the same protocol described above and the best poses also selected for the further MD simulations and MM-PBSA calculations. The interaction energies of the ligands found inside the crystallographic structures listed in Table 1 were also determined using MVD® for reference purposes.

Molecular dynamics simulations

The molecular dynamics (MD) simulations studies were performed applying the bonded and non-bonded parameters for the all-atom force field OPLS-AA (Kaminski et al., 2001). The three-dimensional coordinates and topologies of the targets listed in Table 1 were generated by the pdb2gmx
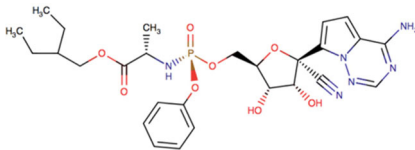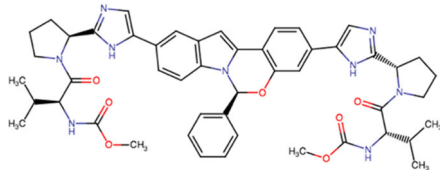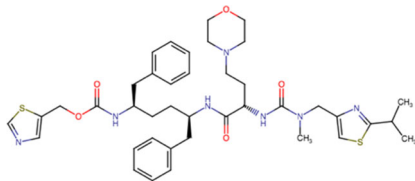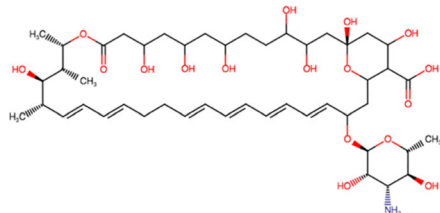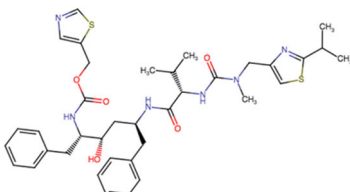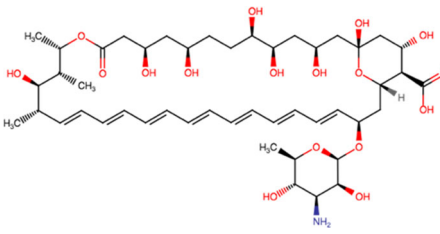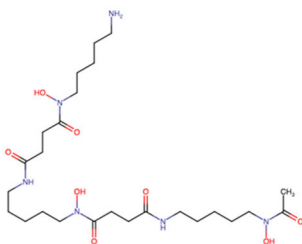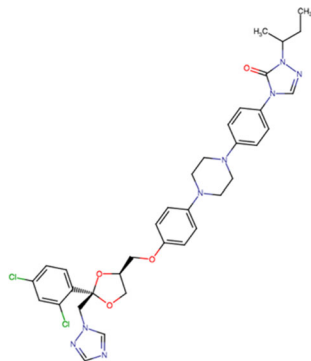
Table 3. Boxes volumes, formats and numbers of water molecules of each system.

Protein name	Box volume (nm³) and format	Number of TIP4P water molecules
SC2Mᵖʳᵒ	849.6, dodecahedron	26,100
SC2SPyke	567.87, dodecahedron	17,671
SC2PLᵖʳᵒ	1204.7, dodecahedron	37,700

software, which is part of the GROMACS 5.1.4 package (Berendsen et al., 1995; Hess et al., 2008; Pronk et al., 2013; Van Der Spoel et al., 2005), used in this work to perform all MD simulations. Since the OPLS-AA force field (Kaminski et al., 2001) has no parameters for the ligands studied, the AcPype software (Sousa Da Silva & Vranken, 2012), was used to generate topology and coordinates files of all ligands submitted to MD simulations. The Restrained Electrostatic Potential (RESP) method (Bayly et al., 1993; Cornell et al., 1993; Ribeiro et al., 2008; Wang et al., 2000) parameterized to reproduce the method Hartree-Fock and the basis set 6-31 G* (Jakalian et al., 2002), was applied to calculate the atomic charges.

The target proteins complexed with the selected ligands were confined inside boxes under periodic boundary conditions (Martínez et al., 2007) where the effect of the solvent was reproduced by the water model TIP4P (Harrach & Drossel, 2014; Jorgensen et al., 1983; Mark & Nilsson, 2001). For each target protein, the box format and size were selected seeking optimization of simulation time and absence of undesired artifacts. The boxes volumes and approximate numbers of water molecules of each system are listed in Table 3. All systems were submitted to two minimization steps using the steepest descent algorithm with the convergence criterion of 100.00 kJ mol⁻¹ nm⁻¹. The first step with position restrained (PR) and the second without PR. The equilibration of pressure and temperature was achieved through 100 ps of simulation using the canonical ensemble (NVT) (Bosko et al., 2005), keeping the number of particles, volume and temperature constant. This was followed by 100 ps of simulation with an isothermal-isobaric ensemble (NPT) (Bosko et al., 2005), keeping the number of particles, pressure, and temperature constant. After the equilibration step, all systems were submitted to a production step of 50 ns. All MD simulations were performed at 310 K and 1 bar, using 2 fs of integration time with the lists of pairs being updated at every 5 steps. The cut-off for Lennard Jones and Coulomb interactions were between 0 and 1.2 nm. The leap-

Table 4. Drugs selected through RBVS plus remdesivir.

Drug	Structure	Drug	Structure
Remdesivir		Elbasvir	
Cobicistat		Nystatin	
Ritonavir		Amphotericin B	
Deferoxamine		Itraconazole	

frog algorithm was used in the production step with the Nose-Hoover thermostat (Evans & Holian, 1985) ($\tau = 0.5$ ps) at 310 K and the Parrinello-Rahman barostat (Parrinello & Rahman, 1981) ($\tau = 2.0$ ps) at 1 bar. All Arg and Lys residues were assigned with positive charges and all Glu and Asp residues were assigned with negative charges. The Visual Molecular Dynamics (VMD) (Humphrey et al., 1996) software was used to visualize the simulation trajectories, and the Grace program (Turner, 2005) was used to build graphs of energy and root mean square deviation (RMSD). Additionally, the same procedure described above was used to run 100 ns of MD simulations with the three crystallographic complexes listed in Table 3, in order to validate our MD simulation protocol.

MM-PBSA calculations

MM-PBSA calculations of the binding free energies of each ligand after the MD simulations were carried out in order to support the former results. Through this method it is possible to predict the binding free energy of the ligands considering the vacuum potential energy, which includes both bonded and nonbonded interactions, as well as the free energy of solvation, which considers both polar and nonpolar terms (Kumari et al., 2014). After MD simulations, the ligands were submitted to the g_mmpbsa tool (Kumari et al., 2014) of GROMACS 5.1.4 package (Berendsen et al., 1995; Hess et al., 2008; Pronk et al., 2013; Van Der Spoel et al., 2005) and their complexes with each target had their binding free energies calculated following the same protocol used before (da Silva et al. 2019; de Almeida et al., 2019).

Results and discussion

Receptor-based virtual screening (RBVS)

The search for potential multitarget drugs returned the 7 drugs listed in Table 4, which have the potential of interacting with all targets listed in Table 1, suggesting that further
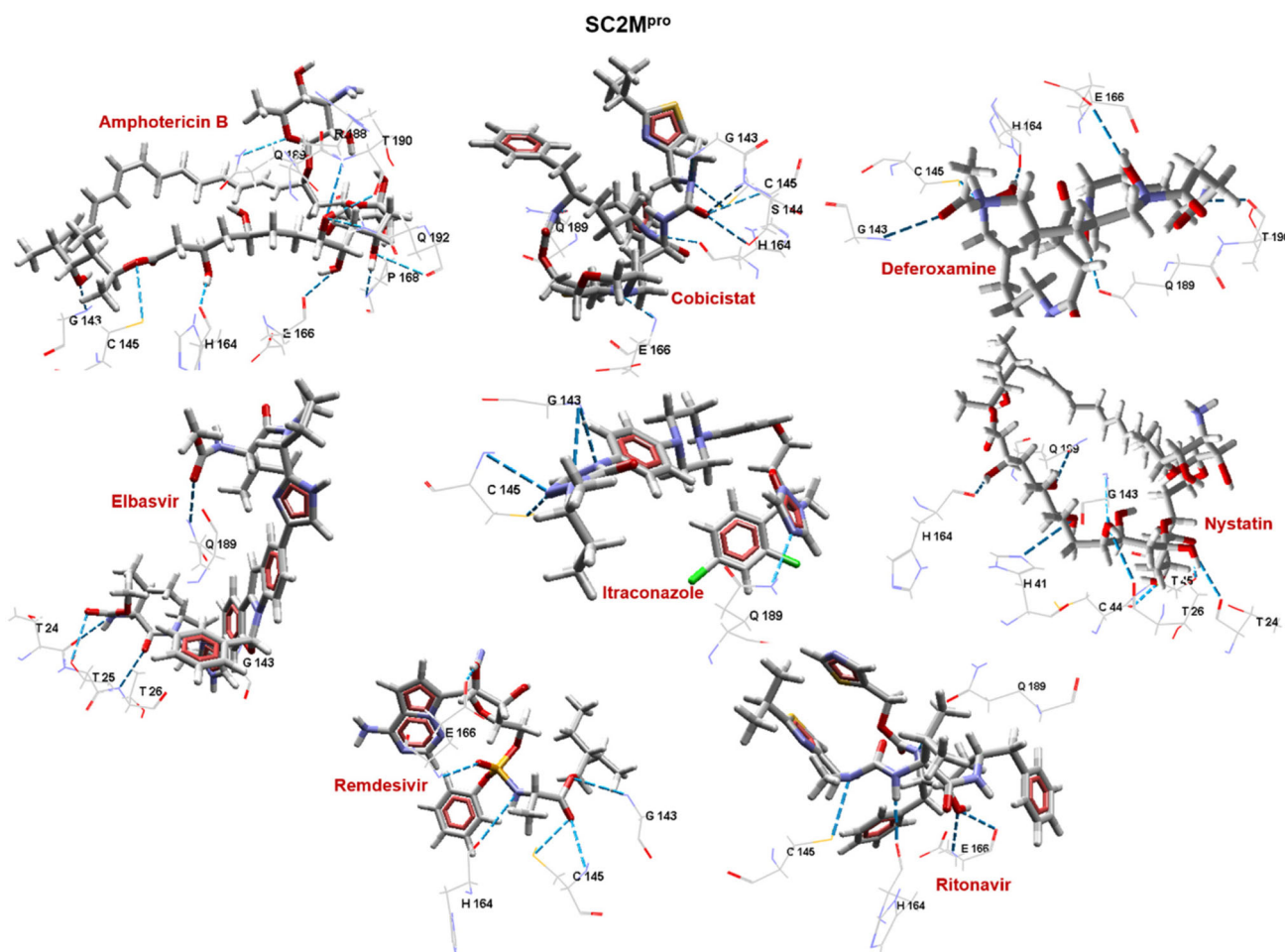
Figure 2. Best pose of each drug inside SC2M^pro. Hydrogen bonds are shown as blue dashed lines.

repurposing studies of those drugs might lead to the discovery of an existing drug with potential to treat COVID-19. The structure of remdesivir is also shown in Table 4.

Some of the drugs presented in Table 4 have very similar structures that justify their similar results. Cobicistat and ritonavir, two antiviral drugs, share several common characteristics as well as nystatin and amphotericin B, which are also very similar to each other. Although having different structures, deferoxamine, itraconazole and elbasvir also showed potential to form stable complexes with all targets. Despite the structural differences, all drugs in Table 4 share the common feature of having several highly electronegative atoms linked to hydrogen atoms, i.e. spots where H-bonds can be formed, which probably contributed to their ability to form stable complexes with multiple proteins.

As mentioned above the 8 drugs presented in Table 4 were submitted to more docking calculations, with each molecular target chosen in this work, using MVD®, so multiple poses per drug per protein could be analyzed regarding their stability.

Docking studies

The results of docking calculations using MVD® shown in Figures 2–5, Table S1 and Figures S1–S25, confirmed the RBVS results, showing that the best poses of all 7 selected drugs are capable of binding to the targets, presenting large negative values of interacting energy (most below -100.00 kcal mol^{-1}) comparable with the results for the reference ligands inside SC2M^pro and SC2PL^pro. In the case SC2Spyke the interaction energy of the reference ligand is not comparable to our ligands once the peptide LCB1 is a much larger ligand. This peptide is capable of establishing many more interactions with the RDB domain of SC2Spyke (see Figure S25), reflecting in the much more negative binding energy value shown in Figure 5. Our ligands, however, presented binding energies with SC2Spyke similar to the other targets which is enough to qualify them as potential good binders to this protein. It was also observed that remdesivir showed similar energy values with all targets. This suggests that it can also qualify as a multi-target drug against SARS-CoV-2. Among the residues observed in interactions with the best poses of each ligand, it's possible to see in the 3D plots of Figures 2–4 and the 2D plots of Figures S1–S24 that most of the residues listed in Table 1 present some kind of interaction with the ligands and, also, that at least one residue of the respective binding site forms H-Bond with the ligand. This confirms that the selected drugs are capable of binding in the binding sites pointed in Table 1 and, therefore, have potential to inhibit the selected targets.
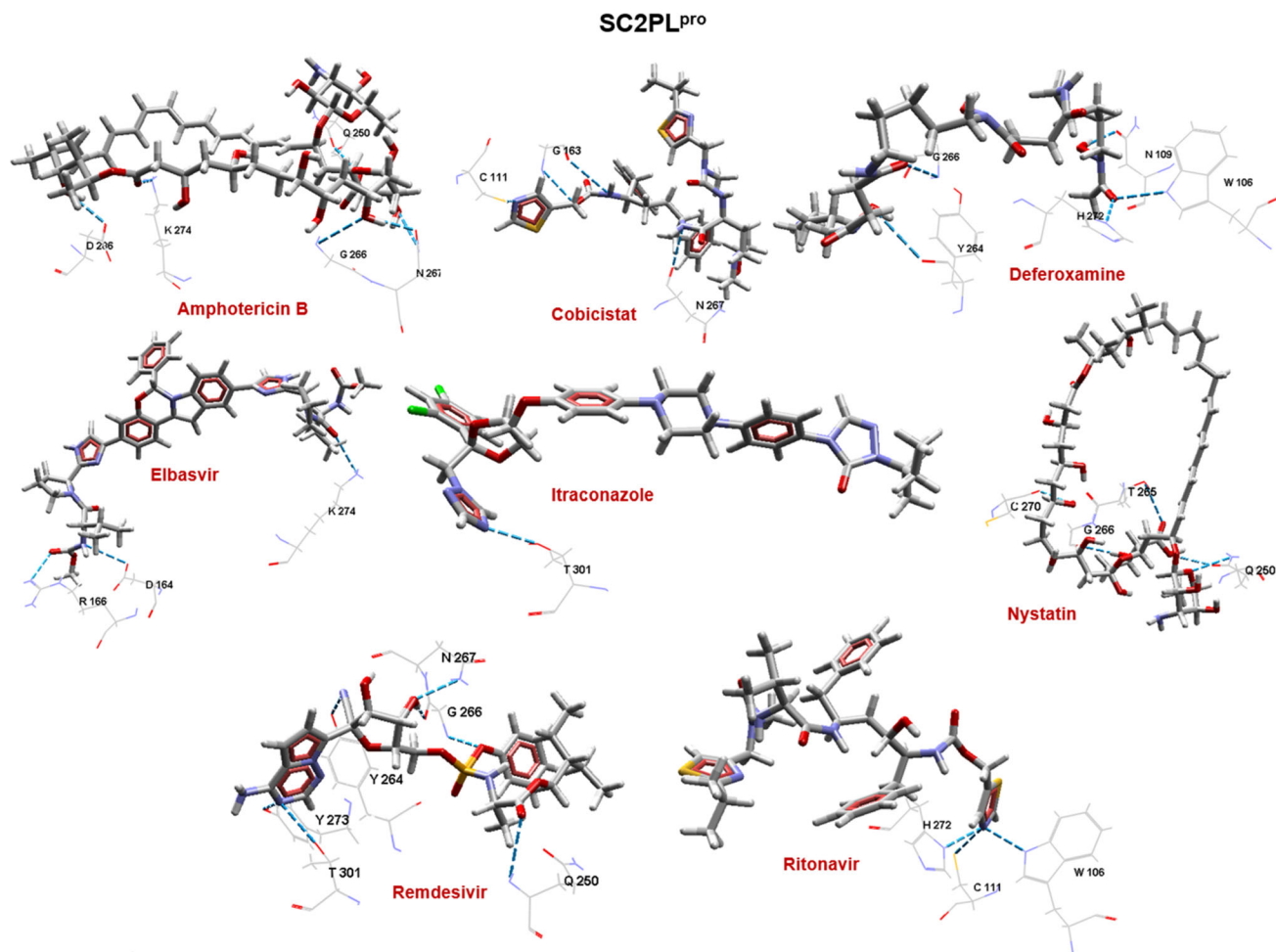
Figure 3. Best pose of each drug inside SC2PL^pro. Hydrogen bonds are shown as blue dashed lines.

Elbasvir was the best binder to all targets according to the docking results, with energy values always below −150 Kcal/mol, while deferoxamine presented the worse (highest) energy values with all targets except *SC2*MPro, where it was the second worse (Table S1). The other 5 ligands presented oscillating results among the targets, ranking well with some and not so well with others.

The selection of the best pose of each drug in each target resulted in 24 systems ligand/target that were submitted to additional rounds of MD simulations and MM-PBSA calculations.

Molecular dynamics simulations

In order to corroborate the docking results, 50 ns of MD simulations were performed with the 24 systems described above (one pose per drug of Table 4 in complex with each protein described in Table 1), plus the three crystallographic complexes listed in Table 3, following the protocol described in the methodology section.

Plots of total and average energy of the crystallographic complexes (Figure S26) show that the systems achieve stability since the beginning of the simulation and allowed reducing the simulated time to 50 ns in order to save computing resources.

Figures S27–S29 and the RMSD of each protein/ligand complex (Figure 6), confirm the stability of the systems during all simulated time. It's possible to see in those figures that the majority of the systems stabilized since the beginning of the MD simulations and that the RMSD of the ligands and proteins never oscillated over 0.7 nm. Deferoxamine and itraconazole were the ligands with worst behavior, showing larger RMSD oscillations with *SC2*Spyke (deferoxamine) and *SC2*M^pro (itraconazole). Elbasvir (shown in blue in Figure 6) behaved well when in complex with all three proteins, indicating the favorable interactions between this ligand and the SARS-CoV-2 targets. Nystatin, shown in pink, presented stable RMSD values specially when complexed with *SC2*PL^pro and *SC2*Spyke. As for *SC2*M^pro, ritonavir (shown in purple) had a good behavior regarding RMSD values; pointing to the possibility of the administration of combined drugs for treating patients with COVID-19. Additionally, remdesivir, which has already shown promising clinical results for COVID-19 treatment (Grein et al., 2020; Hendaus, 2020; Naik et al., 2020; Wang et al., 2020), seems to form more stable complexes with *SC2*PL^pro and *SC2*Spyke than with *SC2*M^pro, enlightening aspects of this drug action regarding SARS-CoV-2. The protein presenting worst behavior was *SC2*M^pro when complexed with amphotericin B.

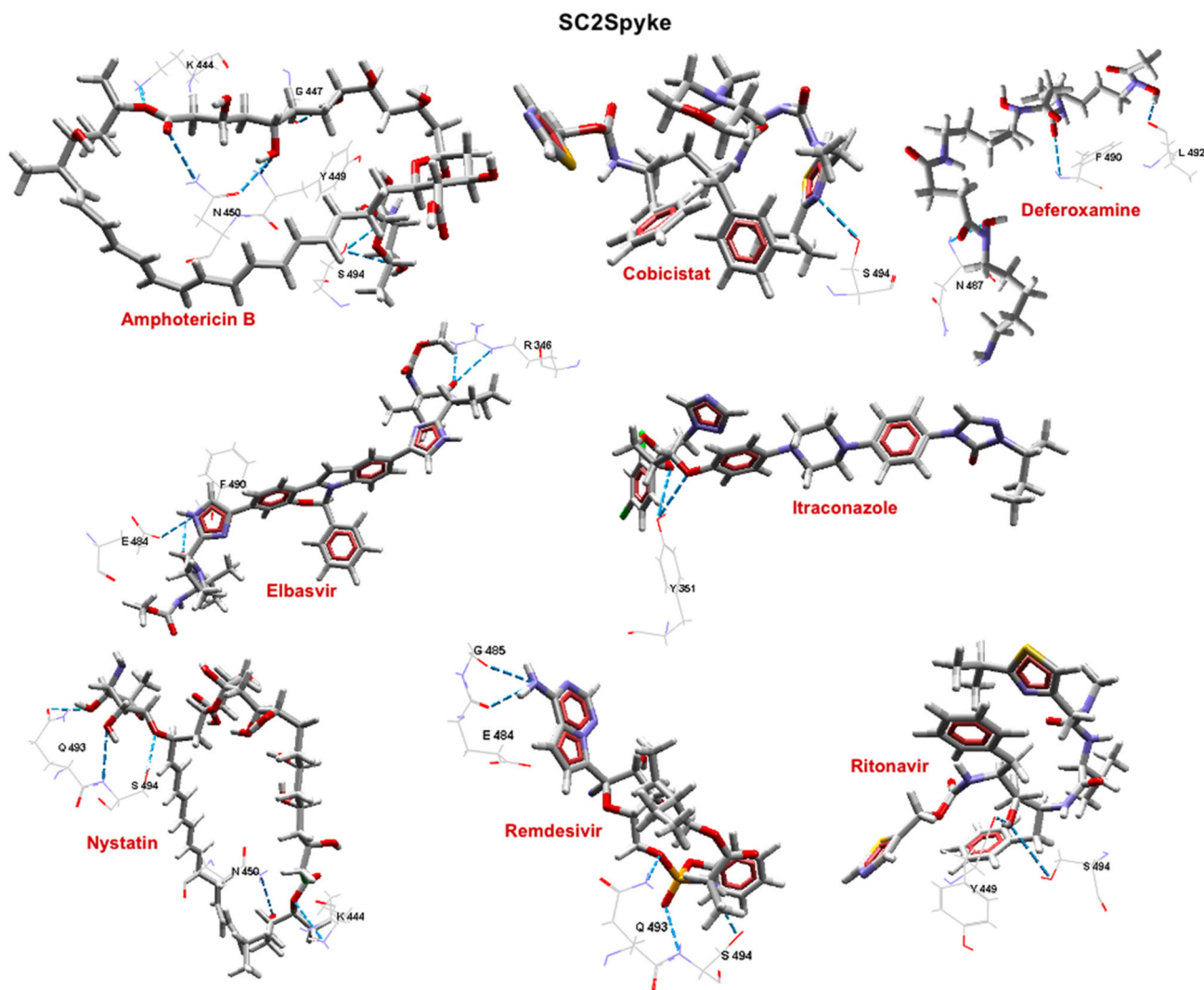The H-bonds formed between each protein and each drug during the MD simulations were also analyzed in order

Figure 4. Best pose of each drug inside SC2Spyke. Hydrogen bonds are shown as blue dashed lines.
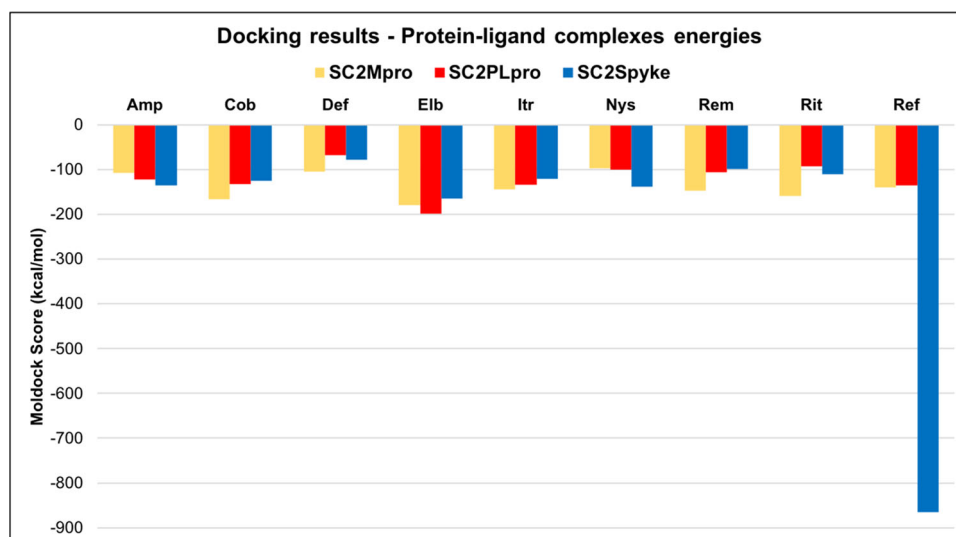

Figure 5. Docking energies (Moldock score) of the best poses of the ligands inside the SARS-CoV-2 targets. Amp: amphotericin B; Cob: cobicistat; Def: deferoxamine; Elb: elbasvir; Itr: itraconazole; Nys: nystatin; Rem: remdesivir; Rit: ritonavir; Ref: Reference ligand.

to verify if such interactions, predicted by docking studies (Figures 2–4), could also be observed during the MD simulations. The reference ligands were also analyzed in this aspect

so the drugs could be compared to them in terms of H-bonds. Figures 7–9 show the H-bonds formed between each molecule and each protein. According to Figure 7, the
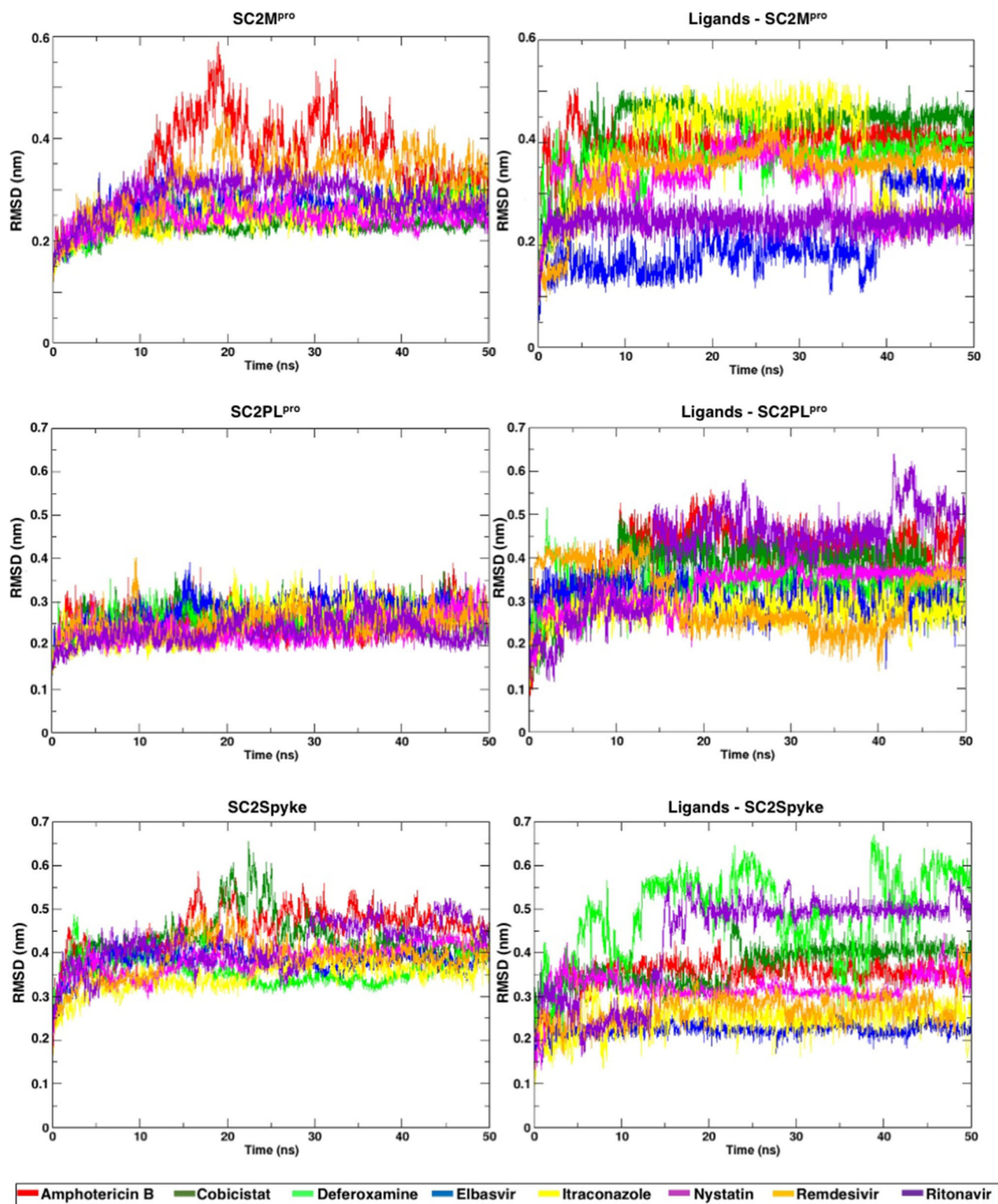
Figure 6. RMSD plots of targets (left) and ligands (right) during 50 ns of MD simulations.

reference ligand to *SC*2M^pro tends to form H-bonds mainly with Glu166 (pink) and Gln189 (green). Amphotericin B, deferoxamine and remdesivir seems to be more promising ligands than the reference in terms of H-bonds, since they interacted with a larger variety of residues during the MD simulations. Regarding interactions with *SC*2PL^pro (Figure 8), elbasvir is not shown because it did not form H-bonds during most of the MD simulation, although this drug presented good docking and RMSD results. As for the other ligands, none seem to be able to form numerous H-bonds with this protein; indicating that there may have non-polar interactions contributing for the complexes stabilities. Remdesivir
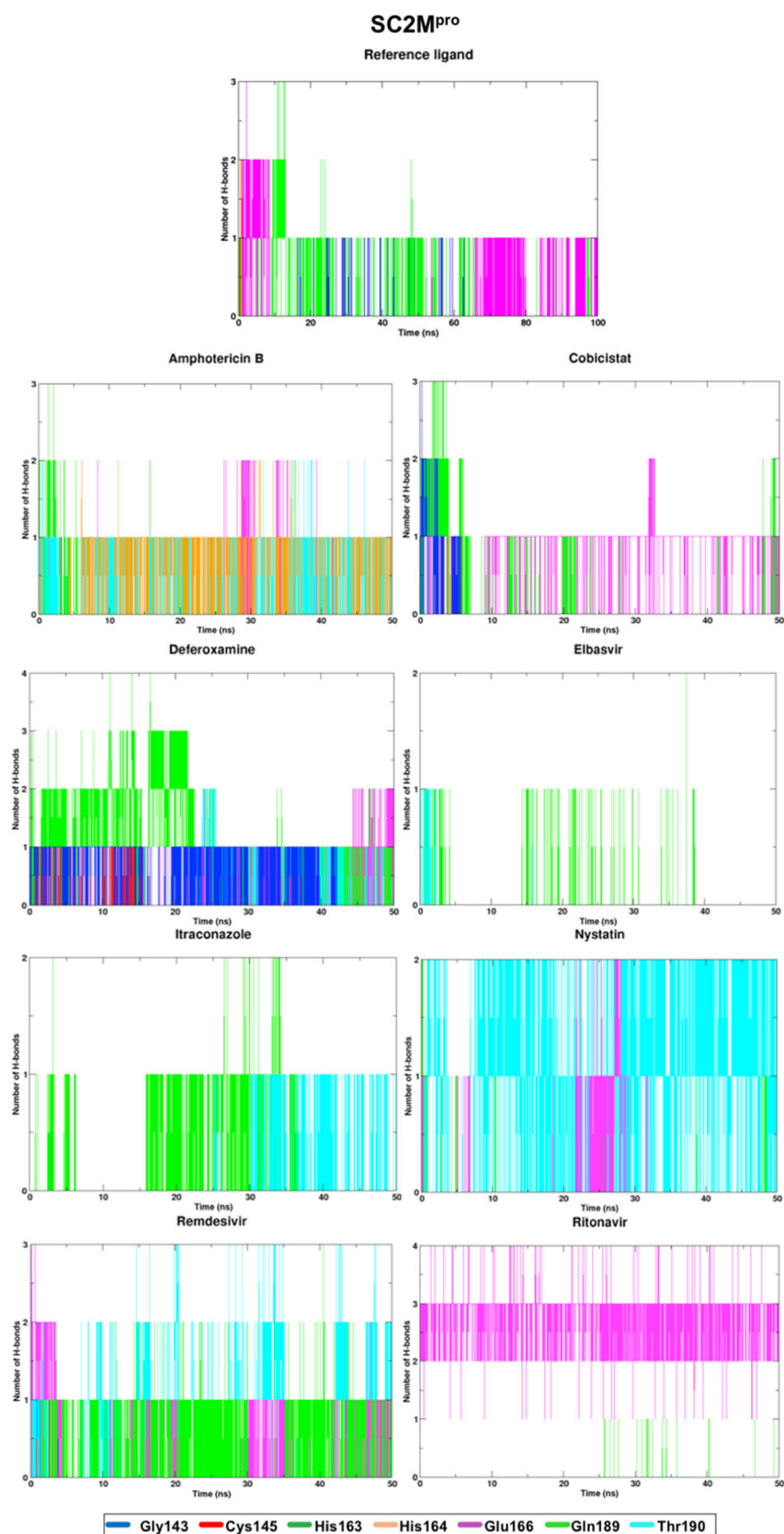
Figure 7. H-bonds formed between *SC2*M^{pro} and the ligands.

seems to be the only drug capable of forming more H-bonds with *SC2*PL^{pro} than the reference ligand. This results contributes to explain the already observed good clinical results of this drug. Considering *SC2*Spyke, Figure 9 shows that most drugs tend to form H-bonds mainly with Tyr449 (red) and Gln493 (blue), while the reference ligand formed H-bonds with multiple residues over the MD simulation time, mainly Lys417 (cyan), Asn487 (dark green), Gly502 (yellow), and
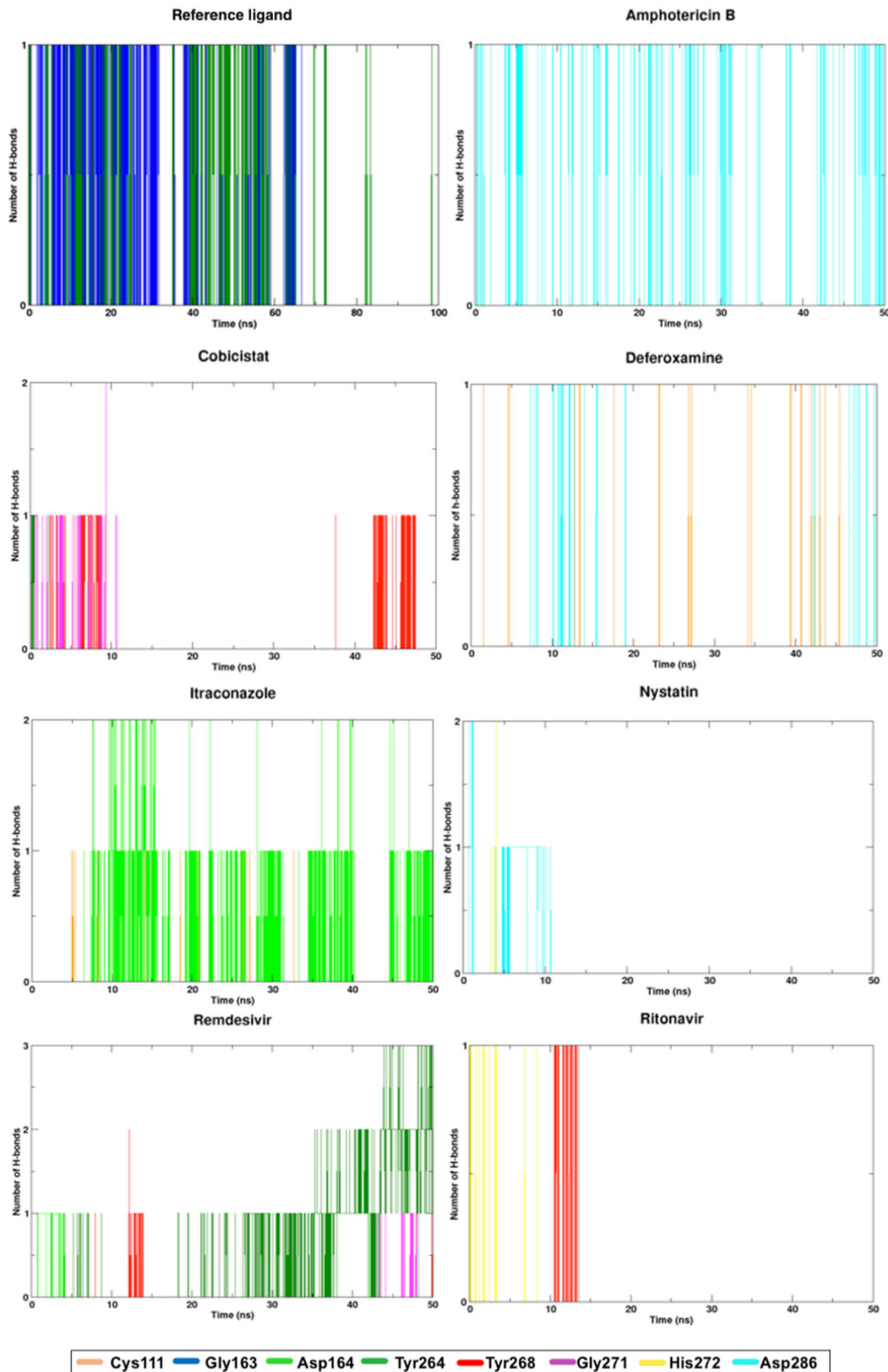
SC2PL^{pro}

Figure 8. H-bonds formed between *SC2*PL^{pro} and ligands. Elbasvir is not shown because it did not form significant H-bonds with this protein.

Tyr449 (red). This is not unexpected since the reference ligand is a peptide and has nearly 60 amino acids (Cao et al., 2020), so its size favors the formation of multiple interactions with *SC2*Spyke residues. Among the studied drugs, deferoxamine, nystatin and remdesivir are the ones that formed H-bonds with *SC2*Spyke residues during most of the MD simulation time, indicating that they tend to stay bound to this protein.
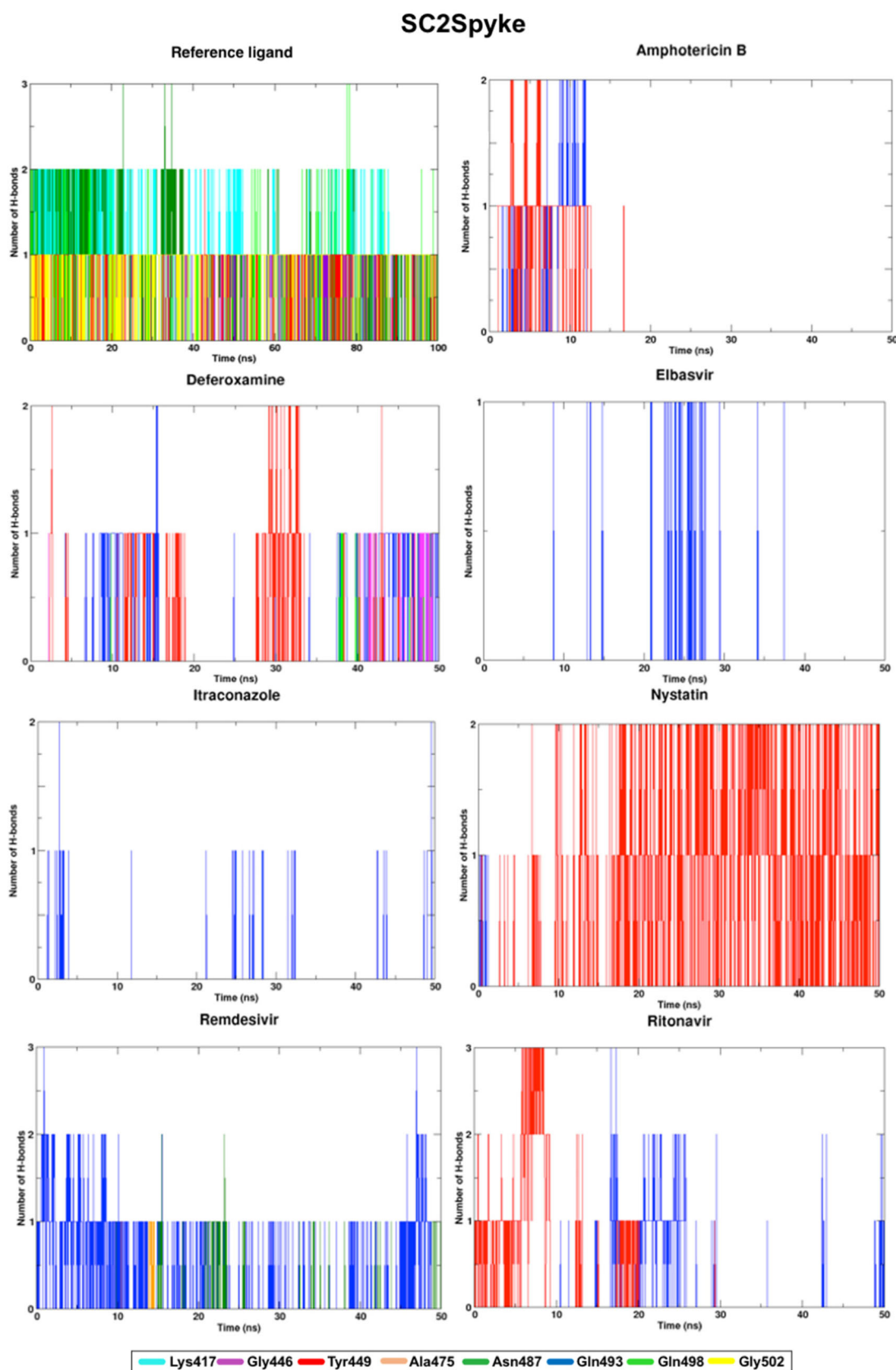
Figure 9. H-bonds formed between *SC2*Spyke and ligands. Cobicistat is not shown because it did not form significant H-bonds with this protein.

MM-PBSA

The results of the MM-PBSA calculations are shown in Figure 10. The negative binding energies predicted for all ligands (most below −50 Kcal mol^{-1}) with all targets corroborated the docking and MD simulations results, confirming their stability and capacity of binding to these targets. Reference ligands of *SC2*M^{pro} and of *SC2*PL^{pro} had similar results to the other drugs, confirming their potential to inhibit those

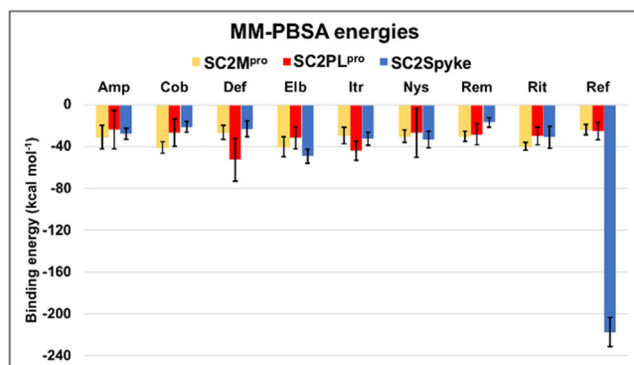**Figure 10.** Plots of MM-PBSA binding energies of drugs and reference molecules bound to SARS-CoV-2 proteins.

proteins. *SC2*Spyke reference ligand presented a significantly lower binding energy than all the other ligands, probably due to its high similarity with the *SC2*Spyke natural substrate (Cao et al., 2020) and consequent extremely low IC_{50} value (Table 3). However, other drugs such as elbasvir, itraconazole, nystatin and ritonavir also had good MM-PBSA results for *SC2*Spyke. Comparing the drug performances for the three proteins, elbasvir and ritonavir are the drugs presenting best general results.

Conclusion

We performed a comprehensive theoretical study applying the methods of RBVS, docking, MD simulations and MM-PBSA calculations, that allowed the selection of 7 potential hits amongst 1930 drugs approved by the FDA (https://chemoinfo.ipmc.cnrs.fr/MOLDB/index.php#ref1). Our 7 hits, together with remdesivir, showed capacity of effectively binding to the three main SARS-CoV2 targets SC2M[pro], SC2PL[pro] and SC2Spyke, qualifying as potential pre-approved multi-target drugs. These results suggest that these drugs, worth being immediately submitted to *in vitro* evaluation against SARS-CoV2. Also, the fact of being multi-target hits suggests that these compounds could have a synergistic effect if administered simultaneously against COVID-19. The most promising drugs for this, according to our results, are remdesivir, elbasvir and ritonavir.

Disclosure statement

No potential conflict of interest was reported by the authors.

Funding

ORCID

Joyce S. F. D. Almeida http://orcid.org/0000-0002-1426-6681
Fernanda D. Botelho http://orcid.org/0000-0001-6407-5800
Felipe R. de Souza http://orcid.org/0000-0001-7410-5188
Marcelo C. dos Santos http://orcid.org/0000-0002-9643-1053
Arlan da Silva Goncalves http://orcid.org/0000-0002-5965-3191
Rodrigo L. B. Rodrigues http://orcid.org/0000-0002-7041-583X
Monique Cardozo http://orcid.org/0000-0002-3918-4287
Daniel A. S. Kitagawa http://orcid.org/0000-0002-6298-0492
Leandro A. Vieira http://orcid.org/0000-0001-9512-2999
Raphael S. F. Silva http://orcid.org/0000-0002-9590-6387
Samir F. A. Cavalcante http://orcid.org/0000-0002-3478-2747
Leonardo da C. Bastos http://orcid.org/0000-0002-9868-9816
Mariana de O. T. Nogueira http://orcid.org/0000-0002-5172-619X
Priscila I. R. de Santana http://orcid.org/0000-0003-1629-4093
Juliana de O. C. Brum http://orcid.org/0000-0003-2039-2075
Eugenie Nepovimova http://orcid.org/0000-0003-0281-246X
Kamil Kuca http://orcid.org/0000-0001-9664-1109
Steven R. LaPlante http://orcid.org/0000-0003-2835-5789
Erick B. F. Galante http://orcid.org/0000-0002-7315-046X
Tanos C. C. Franca http://orcid.org/0000-0002-6048-8103

References

Báez-Santos, Y. M., St. John, S. E., & Mesecar, A. D. (2015). The SARS-coronavirus papain-like protease: Structure, function and inhibition by designed antiviral compounds. *Antiviral Research*, 115, 21–38. https://doi.org/10.1016/j.antiviral.2014.12.015

Bayly, C. C. I., Cieplak, P., Cornell, W. D., & Kollman, P. a. (1993). A well-behaved electrostatic potential based method using charge restraints for deriving atomic charges: The RESP model. *The Journal of Physical Chemistry*, 97(40), 10269–10280. https://doi.org/10.1021/j100142a004

Bedford, J., Enria, D., Giesecke, J., Heymann, D. L., Ihekweazu, C., Kobinger, G., Lane, H. C., Memish, Z., Oh, M-d., Sall, A. A., Schuchat, A., Ungchusak, K., & Wieler, L. H. (2020). COVID-19: towards controlling of a pandemic. *The Lancet*, 395(10229), 1015–1018. https://doi.org/10.1016/S0140-6736(20)30673-5

Berendsen, H. J. C., Van der Spoel, D., & Van Drunen, R. (1995). GROMACS: A message-passing parallel molecular dynamics implementation. *Computer Physics Communications*, 91(1–3), 43–56. nohttps://doi.org/10.1016/0010-4655(95)00042-E

Berman, H. M., Westbrook, J., Feng, Z., Gilliland, G., Bhat, T. N., Weissig, H., Shindyalov, I. N., Bourne, P. E. (2000b). *The protein data bank*. Nucleic acids research. Vol. 28. http://www.rcsb.org/pdb/status.html.

Berman, H. M., Westbrook, J., Feng, Z., Gilliland, G., Bhat, T. N., Weissig, H., Shindyalov, I. N., & Bourne, P. E. (2000a). The protein data bank. *Nucleic Acids Research*, 28(1), 235–242. https://doi.org/10.1093/nar/28.1.235

Bosko, J. T., Todd, B. D., & Sadus, R. J. (2005). Molecular simulation of dendrimers and their mixtures under shear: Comparison of isothermal-isobaric (NpT) and isothermal-isochoric (NVT) ensemble systems. *The Journal of Chemical Physics*, 123(3), 034905. https://doi.org/10.1063/1.1946749

Botelho, F. D., dos Santos, M. C., da S. Gonçalves, A., Kuca, K., Valis, M., LaPlante, S. R., França, T. C. C., & de Almeida, J. S. F. D. (2020, November 26). Ligand-based virtual screening, molecular docking, molecular dynamics, and MM-PBSA calculations towards the identification of potential novel ricin inhibitors. *Toxins*, 12(12), 746. https://www.mdpi.com/2072-6651/12/12/746. https://doi.org/10.3390/toxins12120746

Cao, L., Goreshnik, I., Coventry, B., Case, J. B., Miller, L., Kozodoy, L., Chen, R. E., Carter, L., Walls, A. C., Park, Y.-J., Strauch, E.-M., Stewart, L., Diamond, M. S., Veesler, D., & Baker, D. (2020). De novo design of picomolar SARS-CoV-2 miniprotein inhibitors. *Science*, 370(6515), 426–431. https://doi.org/10.1126/science.abd9909

Cornell, W. D., Cieplak, P., Bayly, C. I., Kollman, P. a., & Kollmann, P. A. (1993). Application of RESP charges to calculate conformational energies, hydrogen bond energies, and free energies of solvation. *Journal*

of the American Chemical Society, *115*(21), 9620–9631. nohttps://doi.org/10.1021/ja00074a030

Cucinotta, D., & Vanelli, M. (2020). WHO declares COVID-19 a pandemic. *Acta Bio-Medica : Atenei Parmensis*, *91*(1), 157–160. https://doi.org/10.23750/abm.v91i1.9397

da Silva, J. A. V., Nepovimova, E., Ramalho, T. C., Kuca, K., & França, T. C. C. (2019, January). Molecular modeling studies on the interactions of 7-methoxytacrine-4-pyridinealdoxime, 4-PA, 2-PAM, and obidoxime with VX-inhibited human acetylcholinesterase: A near attack conformation approach. *Journal of Enzyme Inhibition and Medicinal Chemistry*, *34*(1), 1018–1029. https://www.tandfonline.com/doi/full/10.1080/14756366.2019.1609953. https://doi.org/10.1080/14756366.2019.1609953

de Almeida, J. S. F. D., Cavalcante, S. F. A., Dolezal, R., Kuca, K., Musilek, K., Jun, D., & França, T. C. C. (2019, May 24). Molecular modeling studies on the interactions of aflatoxin B1 and its metabolites with the peripheral anionic site of human acetylcholinesterase. *Journal of Biomolecular Structure & Dynamics*, *37*(8), 2041–2048. http://www.ncbi.nlm.nih.gov/pubmed/29749305. https://doi.org/10.1080/07391102.2018.1475259

Douguet, D. (2010). E-LEA3D: A computational-aided drug design web server. *Nucleic Acids Research*, *38*(Web Server), W615–621. https://doi.org/10.1093/nar/gkq322

Douguet, D. (2018). Data sets representative of the structures and experimental properties of FDA-approved drugs. *ACS Medicinal Chemistry Letters*, *9*(3), 204–209. https://doi.org/10.1021/acsmedchemlett.7b00462

Evans, D. J., & Holian, B. L. (1985). The nose-hoover thermostat. *The Journal of Chemical Physics*, *83*(8), 4069–4074. https://doi.org/10.1063/1.449071

Fierabracci, A., Arena, A., & Rossi, P. (2020). COVID-19: A review on diagnosis, treatment, and prophylaxis. *International Journal of Molecular Sciences*, *21*(14), 5145. https://doi.org/10.3390/ijms21145145

Gao, X., Qin, B., Chen, P., Zhu, K., Hou, P., Wojdyla, J. A., Wang, M., & Cui, S. (2020). Crystal Structure of SARS-CoV-2 papain-like protease. *Acta Pharmaceutica Sinica B*, https://doi.org/10.1016/j.apsb.2020.08.014

Gates, B. (2020). Responding to Covid-19 - A once-in-a-century pandemic? *The New England Journal of Medicine*, *382*(18), 1677–1679. https://doi.org/10.1056/NEJMp2003762

Grein, J., Ohmagari, N., Shin, D., Diaz, G., Asperges, E., Castagna, A., Feldt, T., Green, G., Green, M. L., Lescure, F.-X., Nicastri, E., Oda, R., Yo, K., Quiros-Roldan, E., Studemeister, A., Redinski, J., Ahmed, S., Bennett, J., Chelliah, D., … Flanigan, T. (2020). Compassionate use of remdesivir for patients with severe Covid-19. *New England Journal of Medicine*, *382*(24), 2327–2336. https://doi.org/10.1056/NEJMoa2007016

Harrach, M. F., & Drossel, B. (2014). Structure and dynamics of TIP3P, TIP4P, and TIP5P water near smooth and atomistic walls of different hydroaffinity. *The Journal of Chemical Physics*, *140*(17), 174501–174514. https://doi.org/10.1063/1.4872239

Hehre, W., Ohlinger, S., Klunzinger, P., Deppmeier, B., Driessen, A., Johnson, J., Ohsan, P. (2006). Spartan'08 Tutorial and User's Guide; Q-CHEM, INC.: Irvine, CA, USA. ISBN 978-1-890661-38-4

Hendaus, M. A. (2020). Remdesivir in the treatment of Coronavirus Disease 2019 (COVID-19): A simplified summary. *Journal of Biomolecular Structure and Dynamics*. https://doi.org/10.1080/07391102.2020.1767691

Hess, B., Kutzner, C., van der Spoel, D., & Lindahl, E. (2008, March). GROMACS 4: Algorithms for highly efficient, load-balanced, and scalable molecular simulation. *Journal of Chemical Theory and Computation*, *4*(3), 435–447. http://pubs.acs.org/doi/abs/10.1021/ct700301q. https://doi.org/10.1021/ct700301q

Humphrey, W., Dalke, A., & Schulten, K. (1996). VDM: Visual molecular dynamics. *Journal of Molecular Graphics*, *14*(1), 33–28. noplates,https://doi.org/10.1016/0263-7855(96)00018-5

Jakalian, A., Jack, D. B., & Bayly, C. I. (2002, December). Fast, efficient generation of high-quality atomic charges. AM1-BCC Model: II. Parameterization and validation. *Journal of Computational Chemistry*, *23*(16), 1623–1641. https://doi.org/10.1002/jcc.10128

Jin, Z., Du, X., Xu, Y., Deng, Y., Liu, M., Zhao, Y., Zhang, B., Li, X., Zhang, L., Peng, C., Duan, Y., Yu, J., Wang, L., Yang, K., Liu, F., Jiang, R., Yang, X., You, T., Liu, X., … Yang, H. (2020). Structure of Mpro from COVID-19 virus and discovery of its inhibitors. *Nature*, *582*(7811), 289–293. (April). https://doi.org/10.1038/s41586-020-2223-y

Jorgensen, W. L., Chandrasekhar, J., Madura, J. D., Impey, R. W., & Klein, M. L. (1983). Comparison of simple potential functions for simulating liquid water. *The Journal of Chemical Physics*, *79*(2), 926–935. https://doi.org/10.1063/1.445869

Kaminski, G., Friesner, R., Tirado-Rives, J., & Jorgensen, W. L. (2001). Evaluation and reparametrization of the OPLS-AA force field for proteins via comparison with accurate quantum chemical calculations on peptides. *The Journal of Physical Chemistry B*, *105*(28), 6474–6487. https://doi.org/10.1021/jp003919d

Klemm, T., Ebert, G., Calleja, D. J., Allison, C. C., Richardson, L. W., Bernardini, J. P., Lu, B. G., Kuchel, N. W., Grohmann, C., Shibata, Y., Gan, Z. Y., Cooney, J. P., Doerflinger, M., Au, A. E., Blackmore, T. R., Heden van Noort, G. J., Geurink, P. P., Ovaa, H., Newman, J., … Komander, D. (2020). Mechanism and inhibition of the papain-like protease, PLpro, of SARS-CoV-2. *The EMBO Journal*, *39*(18), 1–17. https://doi.org/10.15252/embj.2020106275

Korb, O., Stützle, T., & Exner, T. E. (2009). Empirical scoring functions for advanced protein-ligand docking with PLANTS. *Journal of Chemical Information and Modeling*, *49*(1), 84–96. https://doi.org/10.1021/ci800298z

Kumari, R., Kumar, R., Lynn, A., & Lynn, A. (2014, July 28). g_mmpbsa-a GROMACS tool for high-throughput MM-PBSA calculations . *Journal of Chemical Information and Modeling*, *54*(7), 1951–1962. http://www.ncbi.nlm.nih.gov/pubmed/24850022. https://doi.org/10.1021/ci500020m

Mark, P., & Nilsson, L. (2001). Structure and dynamics of the TIP3P, SPC, and SPC/E water models at 298 K. *The Journal of Physical Chemistry A*, *105*(43), 9954–9960. https://doi.org/10.1021/jp003020w

Martínez, L., Borin, I. A., & Skaf, M. S. (2007). Fundamentos de Simulação Por Dinâmica Molecular. In N. H. Morgon & K. Coutinho (Eds.), *Métodos de Química Teórica e Modelagem Molecular* (pp. 413–452). Livraria da Física.

Naik, V. R., Munikumar, M., Ramakrishna, U., Srujana, M., Goudar, G., Naresh, P., Kumar, B. N., & Hemalatha, R. (2020). Remdesivir (GS-5734) as a therapeutic option of 2019-NCOV main protease – in silico approach. *Journal of Biomolecular Structure and Dynamics*. https://doi.org/10.1080/07391102.2020.1781694

Ortiz-Prado, E., Simbaña-Rivera, K., Gómez- Barreno, L., Rubio-Neira, M., Guaman, L. P., Kyriakidis, N. C., Muslin, C., Jaramillo, A. M. G., Barba-Ostria, C., Cevallos-Robalino, D., Sanches-SanMiguel, H., Unigarro, L., Zalakeviciute, R., Gadian, N., & López-Cortés, A. (2020). Clinical, molecular, and epidemiological characterization of the SARS-CoV-2 virus and the Coronavirus disease 2019 (COVID-19), a comprehensive literature review. *Diagnostic Microbiology and Infectious Disease*, *98*(1), 115094. https://doi.org/10.1016/j.diagmicrobio.2020.115094

Parrinello, M., & Rahman, A. (1981). Polymorphic transitions in single crystals: A new molecular dynamics method. *Journal of Applied Physics*, *52*(12), 7182–7190. https://doi.org/10.1063/1.328693

Pronk, S., Páll, S., Schulz, R., Larsson, P., Bjelkmar, P., Apostolov, R., Shirts, M. R., Smith, J. C., Kasson, P. M., van der Spoel, D., Hess, B., & Lindahl, E. (2013). GROMACS 4.5: A high-throughput and highly parallel open source molecular simulation toolkit. *Bioinformatics (Oxford, England))*, *29*(7), 845–854. https://doi.org/10.1093/bioinformatics/btt055

Pushpakom, S., Iorio, F., Eyers, P. A., Escott, K. J., Hopper, S., Wells, A., Doig, A., Guilliams, T., Latimer, J., McNamee, C., Norris, A., Sanseau, P., Cavalla, D., & Pirmohamed, M. (2019, December 28). Drug repurposing: Progress, challenges and recommendations. *Nature Reviews. Drug Discovery*, *18*(1), 41–58. https://doi.org/10.1038/nrd.2018.168

Rathnayake, A. D., Zheng, J., Kim, Y., Perera, K. D., Mackin, S., Meyerholz, D. K., Kashipathy, M. M., Battaile, K. P., Lovell, S., Perlman, S., Groutas, W. C., & Chang, K.-O. (2020). 3C-like protease inhibitors block coronavirus replication in vitro and improve survival in MERS-CoV–infected mice. *Science Translational Medicine*, *12*(557), eabc5332. https://doi.org/10.1126/scitranslmed.abc5332

Reed, A. E., Weinstock, R. B., & Weinhold, F. (1985). Natural population analysis. *The Journal of Chemical Physics*, *83*(2), 735–746. https://doi.org/10.1063/1.449486

Ribeiro, A. A. S. T., Horta, B. A. C., & de Alencastro, R. B. (2008). MKTOP: A program for automatic construction of molecular topologies. *Journal*

of the Brazilian Chemical Society, 19(7), 1433–1435. http://www. scielo. br/scielo.php?script=sci_arttext&pid=S0103-50532008000700031&lng= en&nrm=iso&tlng=en. https://doi.org/10.1590/S0103-50532008000700031

Sousa Da Silva, A. W., & Vranken, W. F. (2012). ACPYPE - Antechamber python parser interface. BMC Research Notes, 5(1), 367. https://doi.org/10.1186/1756-0500-5-367

Stewart, J. J. P. (2004). Optimization of parameters for semiempirical methods IV: Extension of MNDO, AM1, and PM3 to more main group elements. Journal of Molecular Modeling, 10(2), 155–164. https://doi.org/10.1007/s00894-004-0183-z

Thomsen, R., & Christensen, M. H. (2006, June 1). MolDock: A new technique for high-accuracy molecular docking. Journal of Medicinal Chemistry, 49(11), 3315–3321. https://doi.org/10.1021/jm051197e

Turner, P. J. (2005). XMGRACE, version 5.1.25. Center for Coastal and Land-Margin Research, Oregon Graduate Institute of Science and Technology.

Van Der Spoel, D., Lindahl, E., Hess, B., Groenhof, G., Mark, A. E., & Berendsen, H. J. C. (2005). GROMACS: Fast, flexible, and free. Journal of Computational Chemistry, 26(16), 1701–1718. https://doi.org/10.1002/jcc.20291

Velavan, T. P., & Meyer, C. G. (2020). The COVID-19 epidemic. Tropical Medicine & International Health : TM & Ih, 25(3), 278–280. https://doi.org/10.1111/tmi.13383

Wang, J., Cieplak, P., & Kollman, P. A. (2000). How well does a restrained electrostatic potential (RESP) model perform in calculating conformational energies of organic and biological molecules? Journal of Computational Chemistry, 21(12), 1049–1074. https://doi.org/10.1002/1096-987X(200009)21:12<1049::AID-JCC3>3.0.CO;2-F

Wang, Y., Zhang, D., Du, G., Du, R., Zhao, J., Jin, Y., Fu, S., Gao, L., Cheng, Z., Lu, Q., Hu, Y., Luo, G., Wang, K., Lu, Y., Li, H., Wang, S., Ruan, S., Yang, C., Mei, C., … Wang, C. (2020). Remdesivir in adults with severe COVID-19: A randomised, double-blind, placebo-controlled, multi-centre trial. The Lancet, 395(10236), 1569–1578. https://doi.org/10.1016/S0140-6736(20)31022-9

Yan, R., Zhang, Y., Li, Y., Xia, L., Guo, Y., & Zhou, Q. (2020, March). Structural basis for the recognition of SARS-CoV-2 by full-length human ACE2. Science (New York, N.Y.).), 367(6485), 1444–1448. https://doi.org/10.1126/science.abb2762